Quantum Electronics **43** (7) 638–645 (2013)

LASER SPECTROSCOPY

PACS numbers: 32.80.Xx; 32.10.Fn; 42.62.Fi
DOI: 10.1070/QE2013v043n07ABEH015175

Role of transient processes in resonance line spectroscopy of caesium atoms in cells with antirelaxation coating

D.I. Sevost'yanov, V.P. Yakovlev, A.N. Kozlov, V.V. Vasil'ev, S.A. Zibrov, V.L. Velichansky

Abstract. **We study the peculiarities of the absorption spectra in $D_{1,2}$-lines of Cs, caused by optical pumping in cells with antirelaxation coating. In these cells the internal state of the atom, which arose under optical pumping by a monochromatic laser field, is preserved with a high probability in a collision with the wall. As a result, the optical pumping action extends to the entire volume of the cell and to all the velocities of the atoms. This leads to the speed-dependent scanning distortions of the absorption line profile. The detected features should be considered when using laser-pumped quantum magnetometers with antirelaxation-coated cells.**

Keywords: *antirelaxation coating, optical pumping, relaxation, Doppler-free spectroscopy.*

1. Introduction

Transitions between hyperfine and magnetic sublevels of the ground state of alkali-metal atoms have been widely used in frequency standards and quantum magnetometry for more than 50 years [1–3]. New progress has been observed in these fields in recent decades [4–7]. The metrological value of quality of radiofrequency and UHF resonances is first of all related to its narrow spectral width. The latter is determined by the relaxation rates for atom collisions with cell walls and each other [3, 8]. There are two ways to make lines narrower. The first way is adding a buffer gas to the cell, which makes the time interval between collisions with a wall longer because a fast ballistic motion of atoms is replaced by slow diffusion. Possibilities of this method are limited by the line broadening due to collisions of alkali atoms with atoms of the buffer gas [7]. The second way is to deposit an antirelaxation coating onto internal walls of the cell, which reduces the probability of relaxation of internal states of atoms in collisions with walls [3, 8]. The coated cells are widely used in quantum magnetometers with optical pumping [4, 5, 8]. As compared to cells with a buffer gas, they provide a better signal-to-noise ratio and weaken an influence of the magnetic field gradient so that the field averaged over the cell volume can be measured.

Resonance lamps on alkali metals are used in commercial quantum magnetometers. In recent years, resonance lamps are actively replaced by diode lasers, which open new possibilities for the double radio-optical resonance method [9]. In particular, diode lasers can simultaneously pump a great number of cells in a magnetocardiograph [10, 11] and minimise the energy consumption and weight of portable magnetometers.

In the present work we employed the cells with antirelaxation coating filled with caesium vapour and a control cell without such a coating. The linewidth of the employed extended cavity diode lasers (~1 MHz) is less than the natural width of resonance lines (~5 MHz), which, in turn, is less than the Doppler width (~380 MHz) of ^{133}Cs-line at room temperature by almost two orders of magnitude. Thus, the laser radiation of a fixed frequency efficiently interacts with only a small (as compared to the whole ensemble of atoms) group of atoms. However, the nonuniform distribution of atoms over sublevels of the ground state caused by optical pumping not only persists in collisions, but is also extended to all other velocity groups including the group of atoms interacting in resonance with the laser field. Here we investigate the influence of this effect on the resonance absorption spectra of a running probe wave and on formation of a Doppler-free structure if there is an oncoming saturating wave in the case of varied rates of laser frequency scanning.

In Section 2, an experimental setup and the results obtained are described. Most of the features of spectra obtained in coated cells are explained in Section 3. A theoretical model describing the effect of the antirelaxation coating is presented in Section 4.

2. Experiment

2.1. Experimental setup

The spectra were recorded by using the tunable extended cavity diode lasers (ECDLs) [12] adjusted to D_1- or D_2-line. D_1-line was detected in the cylindrical cell with antirelaxation coating of length 72 mm, and diameter 50 mm filled with cae-

D.I. Sevost'yanov, V.P. Yakovlev National Research Nuclear University 'MEPhI', Kashirskoye shosse 31, 115409 Moscow, Russia; e-mail: demetrius37@yandex.ru, yakovlev@theor.mephi.ru;
A.N. Kozlov N.V. Pushkov Institute of Terrestrial Magnetism, Ionosphere and Radio Wave Propagation, Russian Academy of Sciences, Kaluzhskoe shosse, 4, 142190 Moscow, Troitsk, Russia; 'Energotsentr' Ltd., ul. Akad. Anokhina, 38, 119602 Moscow, Russia; e-mail: kozlov@izmiran.ru;
V.V. Vasil'ev, S.A. Zibrov P.N. Lebedev Physics Institute, Russian Academy of Sciences, Leninsky prosp. 53, 119991 Moscow, Russia; e-mail: vvv@okb.lpi.throitsk.ru, szibrov@yandex.ru;
V.L. Velichansky National Research Nuclear University 'MEPhI', Kashirskoye shosse 31, 115409 Moscow, Russia; 'Energotsentr' Ltd., ul. Akad. Anokhina, 38, 119602 Moscow, Russia; P.N. Lebedev Physics Institute, Russian Academy of Sciences, Leninsky prosp. 53, 119991 Moscow, Russia; Russian Quantum Centre, ul. Novaya 100, 143025 Skolkovo, Moscow region, Russia;
e-mail: vlvlab@okb.lpi.throitsk.ru

Received 14 March 2013; revision received 12 April 2013
Kvantovaya Elektronika **43** (7) 638–645 (2013)
Translated by N.A. Raspopov

sium vapour. Characteristics of D_2-line were recorded by using a shorter coated cell with the length of 51 mm and diameter of 36 mm. For revealing the effect of the coating, reference spectra of caesium vapour were recorded in the cell without antirelaxation coating.

The frequency of laser emission was scanned by applying a saw-like voltage across the piesoceramic element controlling the diffraction grating [12]. The modulation frequency varied from 0.1 to 100 Hz and the laser emission frequency variation was 1–5 GHz. This provided recording of the Doppler profile in time intervals from dozens of seconds to milliseconds at raising or falling the laser radiation frequency. The laser radiation passed through an optical isolator, half-wavelength plate, and polariser (not shown in the scheme), which provided a control of the laser power. The linearly polarised emission having passed through a semi-transparent mirror M1 entered the optical system for Doppler-free spectroscopy (Fig. 1). In position 1, Doppler-free resonances were observed against the background of the Doppler profile at the ratio of pumping to probe beam intensities 3:1. Absorption of running wave radiation was detected in position 2.

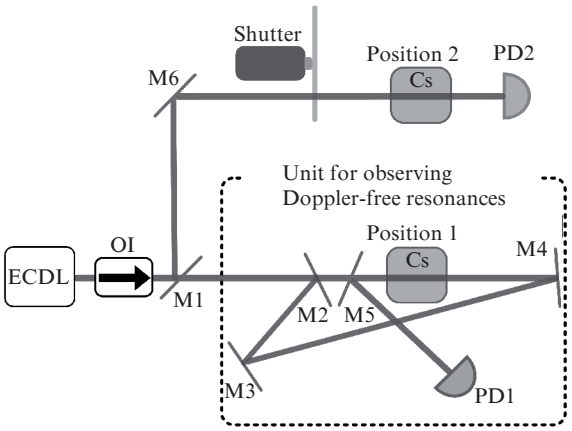

Figure 1. Experimental setup: (ECDL) extended cavity diode laser; (OI) optical isolator; (M1, M2, M5) semi-transparent mirrors; (M3, M4, M6) highly reflecting mirrors; (PD1, PD2) photodetectors.

2.2. Results for D_1-line

In the spectrum of D_1-line of Cs single hyperfine transitions can be studied because the lines of all the four transitions $6S_{1/2}$, $F_g = 3, 4 \rightarrow 6P_{1/2}$, $F_e = 3, 4$ are resolved: at the Doppler line broadening of ~0.38 GHz, the interval between hyperfine sublevels for the ground state is 9.2 GHz and for the excited state it is 1.2 GHz (Fig. 2). In the experiment we chose the transition $F_g = 3 \rightarrow F_e = 4$, in which the nonlinearity due to the pumping to the other hyperfine sublevel $F_g = 4$ dominates, and redistribution over magnetic sublevels has negligible influence.

The insertion in Fig. 2 shows transient characteristics of caesium cell transmission under a stepwise onset of the laser radiation of various intensities at the fixed frequency corresponding to a centre of the transition $6S_{1/2}$, $F_g = 3 \rightarrow 6P_{1/2}$, $F_e = 4$. The laser field was periodically switched on by a mechanical chopper. The front of the light pulse was at most 0.1 ms, the time between the pulses was sufficient for complete relaxation of atoms in the cell. The photodetector response time was less than 10 ms. In Fig. 2 one can see that

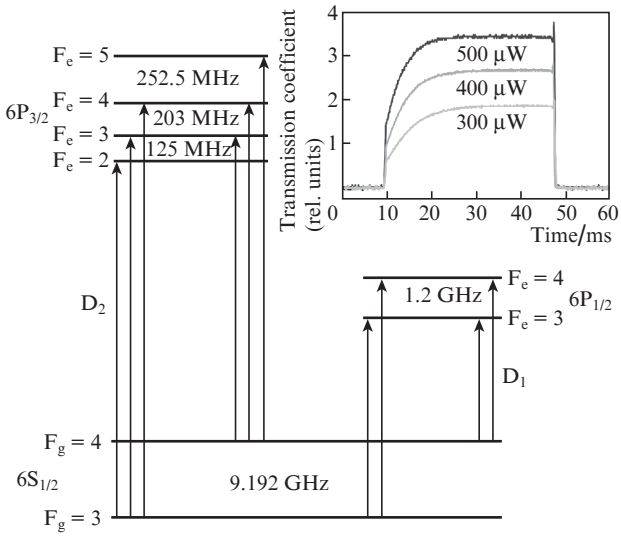

Figure 2. Schematic diagram of levels and allowed transitions for D_1- and D_2-lines of Cs atom. Inset: time dependences of the cell transmission at the central frequency of the laser field at various radiation powers (the beam cross section is $\sim 2 \times 3$ mm).

the time needed to reach a steady-state transmission is longer than 10 ms and increases with decreasing laser radiation power. This time is much longer than the time needed for atom to flight across the beam, which equals to $\sim 2 \times 10^{-5}$ s.

The transmission coefficients for the probe wave and coated cell in position 1 are juxtaposed in Fig. 3 to those for the cell without a coating in position 2. One can see that in the case of coated cell 1) the minimal transmission coefficient for the probe wave is observed earlier than in the cell without coating, 2) a Doppler-free resonance is detected with a high contrast despite the fact that the pumping selectivity with respect to atom longitudinal velocity is lost in collisions with the walls, and 3) the position of the Doppler-free resonance corresponds to the minimum of the background profile of transmission coefficient in a cell without a coating.

The time dependences of the transmission coefficients for the coated cell in position 1 shown in Fig. 4 were recorded at raising and falling frequencies of the probe

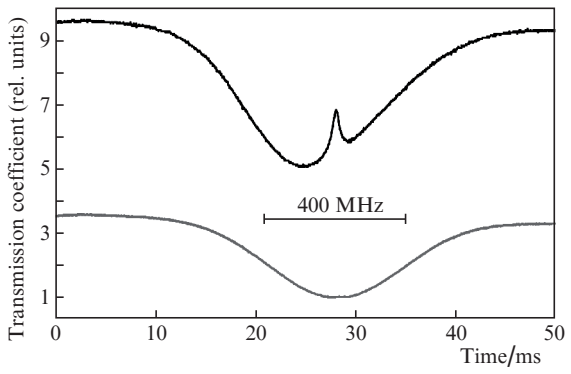

Figure 3. Time evolution of the transmission on the $F_g = 3 \rightarrow F_e = 4$ transition of Cs atom for the coated cell in position 1 (upper curve) and for the uncoated cell in position 2 (bottom curve).

field. The scanning rate was 30 MHz ms^{-1}. A change of sign of frequency tuning corresponds to the vertical dashed line. In both cases one can clearly see the shift of the minimum of the background transmission relative to the Doppler-free resonance and violation of the profile symmetry. The character of the distortion depends on time and not on the sign of frequency tuning. From the position of the Doppler-free resonance one can find the instant when the frequency of laser radiation corresponds to a maximum of the Maxwellian distribution of atoms over longitudinal velocity. Note that the saturating field not only forms a Doppler-free resonance but also substantially distorts the background profile because it is more intensive than the probe wave.

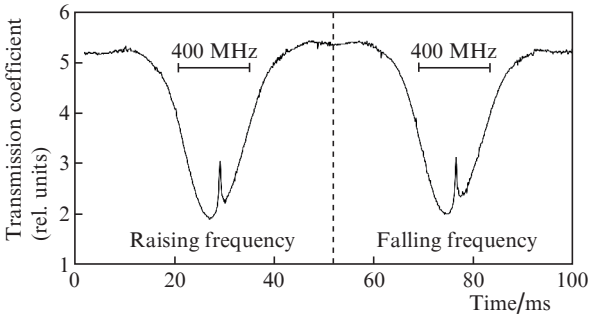

Figure 4. Transmission on the $F_g = 3 \rightarrow F_e = 4$ transition for D_1-line of Cs atom for the cell with coating in position 1 in the cases of raising and falling frequencies of the probe field. The pump radiation intensity is ~1 mW cm^{-2}.

The shift of the Doppler-free resonance relative to the minimum of the Doppler-broadened transmission profile is observed in a wide range of frequency tuning rates (from ~1 GHz ms^{-1} to ~1 MHz ms^{-1}). Near the ends of this range the shift is negligible (Fig. 5). It takes a maximum value at the scanning rate of ~50 MHz ms^{-1}.

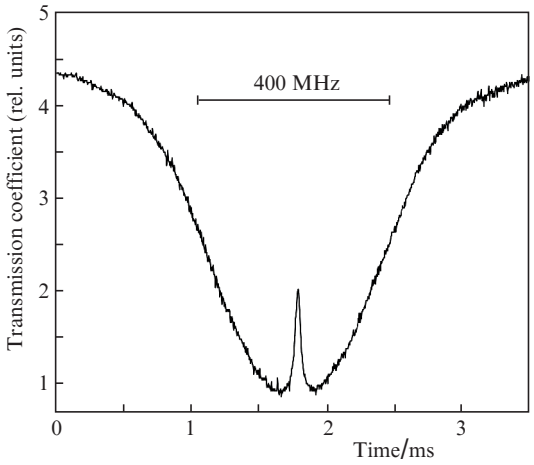

Figure 5. Transmission on the $F_g = 3 \rightarrow F_e = 4$ transition for D_1-line of Cs atom for the coated cell in position 1 under fast (~300 MHz ms^{-1}) frequency scanning. The pump radiation intensity is ~1 mW cm^{-2}.

2.3. Results for D_2-line

Due to Doppler broadening, six hyperfine components of Cs D_2-line $6S_{1/2}$, $F_g = 3,4 \rightarrow 6P_{3/2}$, $F_e = 2,3,4,5$ (see Fig. 2) merge into two lines. Each of the lines corresponds to three hyperfine transitions two of which are cyclic in quantum number F. The specificity of transmission spectra caused by antirelaxation coating is more pronounced in the long-wavelength group of transitions $F_g = 4 \rightarrow F_e = 3,4,5$ (Fig. 6). The distortions of D_1-line depends on the frequency scanning rate, whereas the situation with D_2-line is quite distinct. The value of maximal absorption (minimal transmission in Fig. 6) in the total profile noticeably differs for different directions of frequency tuning. Under frequency reduction where the absorption on a cyclic transition starts first, a greater maximal absorption is reached. Note that all the Doppler-free resonances (three at eigenfrequencies and three crossovers) are allowed.

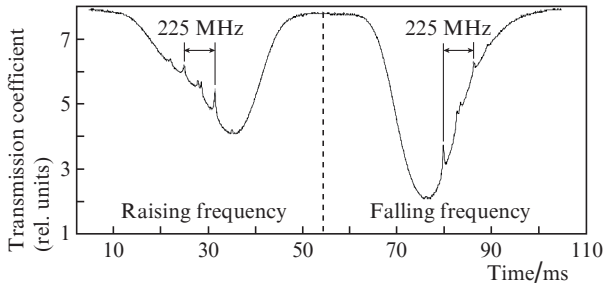

Figure 6. Transmission spectrum for D_2-line (transitions $F_g = 4 \rightarrow F_e = 3, 4, 5$) for the coated cell in position 1 in the cases of raising and falling frequencies of the laser radiation. The pump radiation intensity is ~1 mW cm^{-2}.

3. Discussion and qualitative explanation of the results

In atoms with a nonzero nucleus spin with a hyperfine (HF) structure of the ground state the nonlinearity in the interaction of laser radiation with an ensemble of atoms may occur not only at noticeable population of the excited state with the lifetime of $\sim 3 \times 10^{-8}$ s, but also in the case where a large part of atoms is transferred to nonabsorbing hyperfine or magnetic sublevels of the ground state. In the second case, the relaxation time for the disturbance is at least the time of flight of atom across the laser beam ($\tau_0 \approx 10^{-5}$ s), and the nonlinearity is revealed at the intensities two–three orders lower than in the case of two-level systems. In magnetometers or atomic clocks, a low-intensity radiation is used to avoid power broadening of metrological resonances. In the present work the intensities were smaller than 1 mW cm^{-2} but sufficient to produce the above-mentioned nonlinearity.

The internal state of the atom colliding with the wall of the coated cell remains constant at a high probability, whereas the projection of the velocity on the laser beam propagation direction changes. Thus, the effect of optical pumping is spread over the entire Maxwellian velocity distribution. As a result, nonlinear interaction of atoms with laser radiation is formed in the following two channels: one is caused by pumping into the nonabsorbing state in a time of flight of atom through the laser beam, the other is related with a return of

such atoms after a single or several collisions with the walls to the laser beam (i.e., to the interaction zone) in a characteristic time τ_v. The probability of the return after a first collision is proportional to the ratio of natural to Doppler line width and to the ratio of beam cross section to the area of the base of the cylindrical cell. In the experiment, this value was not above 10^{-2}.

For the second channel, there is an effect of atom accumulation in the nonabsorbing state, which results in increasing the degree of nonlinearity during the time when the laser frequency remains within the limits of Doppler-broadened line profile. If this time is longer than the time of attaining a stationary regime for the whole ensemble of atoms $T = \tau_g/(1+P\tau_g)$ (where τ_g is the population relaxation time for hyperfine sublevels of the ground state, P is the rate of atom transfer into the nonabsorbing state) then the absorption stops changing. This simple estimate is valid for moderate radiation intensities and pumping rates, because T cannot be shorter than the time of flight of atom across the laser beam. The dynamics of the pumping is analysed in more details in the next Section. Passing to a stationary level means that the distribution of population was established for the whole ensemble of atoms over both volume and velocities. It is for this reason that the transient period of cell constant transmission ($\sim$0.01 s) recorded at a fixed probe radiation frequency and presented in Fig. 2 is much longer than the time of flight of atom across the laser beam (2×10^{-5} s), which determines the transient period of stationary absorption for cells without a coating.

In the frequency scanning regime, absorption in each point of Doppler profile (in each velocity group) is determined by the action of the field on other velocity groups of atoms in preceding instants. At certain rates of frequency tuning (see below) the absorption due to the delayed action of pumping in the second channel depends on interaction processes at preceding instants, which results in distortions of the line profile observed. Note that the change in frequency may be not only linear (in recording a spectrum) or harmonic (in forming the error signal for laser frequency stabilisation system) but can stem from fluctuation.

In scanning the laser frequency within the Doppler profile at a rate of $\sim$100 MHz ms^{-1} atoms are accumulated in the nonabsorbing state during the whole time needed to pass the Doppler-broadened line. At the stage where the laser frequency tunes from the line tail to its centre, the raising function of the atom distribution over the longitudinal velocity is multiplied by a decreasing function due to the total accumulation of nonabsorbing atoms. This is why the minimum transmission is attained prior to the moment when the laser frequency becomes equal to the central frequency of the Maxwellian distribution (see Fig. 3). For solitary, hence, symmetrical hyperfine components of D_1-line the effect is independent of the sign of frequency tuning, which is confirmed in Fig. 4.

At a high scanning rate (Fig. 5), where the time of line scanning is noticeably shorter than T, the influence of the second channel (the degree of pumping of the entire ensemble of atoms) is small even at the end of the scanning because the shift of the background transmission extremum relative to the undisturbed atomic frequency vanishes. The same situation occurs under a very slow frequency scanning ($\sim\gamma/T$ = 5 MHz ms^{-1} = 0.5 GHz s^{-1}, where γ is the natural line width) because the ensemble of atoms manages to approach the stationary state at each frequency value. Obviously, there exists the rate of tuning at which the shift of the transmission profile minimum relative to the centre of the Maxwellian distribution takes a maximum. The dependence shown in Fig. 3 corresponds to this case.

Revert to the features of D_2-line transmission, where all six HF components merge into two groups each comprising three HF components. The profile distortions due to the antirelaxation coating are more pronounced in the long-wavelength group ($F_g = 4 \rightarrow F_e = 3, 4, 5$), for which the corresponding experimental curves are presented in Fig. 6. As was mentioned the character of D_2-line distortion noticeably differs from that for D_1-line. The maximal absorption in the total profile depends on the sign of frequency tuning. As the laser radiation frequency approaches that of the transition $F_g = 4 \rightarrow F_e = 3, 4, 5$ from the long-wavelength side, open transitions first fall in resonance with the field. In the result, the transfer of atoms to the 'dark' HF sublevel $F_g = 3$ noticeably empties the level $F_g = 4$ up to the moment when the laser radiation frequency approaches the center of the most intensive HF component$F_g = 4 \rightarrow F_e = 5$ in the triplet. This is why the maximal absorption is noticeably weaker in this case than in scanning the line from the short-wavelength side where the first transition that fits resonance is the cyclic transition $F_g = 4 \rightarrow F_e = 5$, which does not produce optical pumping and is most intensive. Note that in the result of the combined open and cyclic transitions other effects also exhibit specific features. Thus, in early work [13] it was noted that just such a combination makes crossed resonances to dominate in the Doppler-free spectrum of the long-wavelength component of Cs D_2-line; in [14] the same combination leads to a maximal amplitude of magneto-optical resonances.

An important item is possible observation of Doppler-free resonances caused by the nonlinearity due to the population redistribution (polarisation) of atoms induced by laser radiation on sublevels of the ground state in coated cells. Indeed, in order a Doppler-free resonance to occur it is necessary that the nonlinearity due to an action of the pump wave was selective with respect to the atom velocity. However, in colliding with cell walls, atoms change the velocity while keeping the induced polarisation, which breaks the selectivity with respect to the longitudinal velocity and may affect the amplitude of the Doppler-free resonance.

The amplitude of a Doppler-free resonance is determined by the difference in absorption coefficients at the resonance frequency and around it (under the detuning of several γ). In the resonance conditions, both pump channels lead to saturation and reduction of absorption, whereas under frequency detuning only the second channel does, due to the return of atoms transferred to the nonabsorbing state after collisions with cell walls. However, it is clear that the degree of saturation determined by the second channel is lower by at least ω_D/γ times because the result of pumping during the time of flight of atoms in the resonance group through the laser beam after collisions with walls is distributed over the whole ensemble of the atoms possessing the Doppler width ω_D. Thus, Doppler-free resonances should be observed in coated cells as well with the contrast comparable to that for a cell without a coating, which was confirmed experimentally.

Note that in magnetometers developed for geology survey, the lasers with the generation linewidth of 50–100 MHz are employed. In addition, a running wave is detected in the magnetometers whereas a backward wave may only arise as a result of parasitic reflection from cell output window. Nevertheless, even in this case one can observe a Doppler-free resonance with a more complicated structure [15]. Appearance

of a narrow structure in the absorption profile may lead to excess noise due to the conversion of phase noise to amplitude.

4. Theoretical model

In analysing the results of experiments we will use a three-level scheme presented in Fig. 7. The optical radiation of frequency $\omega = \omega_{31} + \Delta$, where ω_{31} is the frequency of transition between levels 3 and 1, Δ is the laser frequency detuning from atom resonance frequency, interacts with the working transition of atom $|1\rangle \leftrightarrows |3\rangle$ and is presented by the pump wave either running along (in the direction of z axis) or accompanied by a weak (probe) oncoming wave. The Rabi frequencies of induced transitions corresponding to these waves satisfy the weak absorption conditions $|\Omega_2| \ll |\Omega_1| \ll \gamma$, where the total width $\gamma = \gamma_1 + \gamma_2$ of the upper level is the sum of partial constants of spontaneous decay in the channels $|3\rangle \to |1\rangle, |2\rangle$.

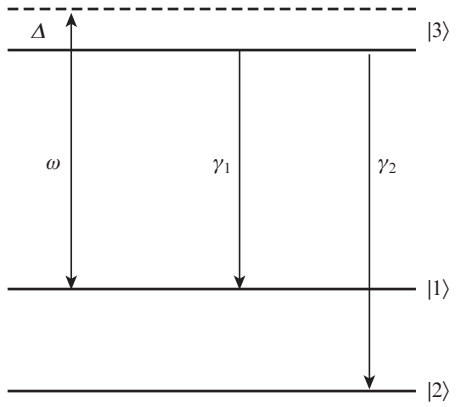

Figure 7. Schematic diagram of levels and transitions in the theoretical model.

The problem has several characteristic times. For simplicity, we may neglect geometrical factors and assume that the interaction of atoms with the laser field occurs during the efficient time τ_0 of particle flight across the laser beam. After the flight atoms collide with cell walls so that the velocity distributions for each of the states $|1\rangle$ and $|2\rangle$ relax in the time τ_v to equilibrium values. The interaction with the laser field substantially depends on the longitudinal (along the beam axis) velocity $v_z \equiv v$, for which the equilibrium distribution function has the form

$$f(v) = \frac{1}{\sqrt{\pi}\, v_T} \exp\left(-\frac{v^2}{v_T^2}\right),$$

where v_T is the thermal velocity. By the order of magnitude τ_v coincides with the average time needed for atom to reach the cell wall and characterises the time of atom return to the laser beam.

Without loss of generality one may assume that τ_v is several times greater than τ_0. Collisions with walls equalise the populations of states $|1\rangle$ and $|2\rangle$, i.e., lead to relaxation of inner states of atoms with a characteristic time τ_g.

In cells without a coating $\tau_g \sim \tau_v$ and we may assume that at times greater than τ_v all the atoms coming into the interaction zone have the equilibrium velocity distribution and equal populations of states $|1\rangle$ and $|2\rangle$. Note that the energy interval between hyperfine sublevels of the ground state is noticeably less than the thermal energy and their populations are proportional to the corresponding statistical weights. A small difference between the statistical weights for $F_g = 3$ and $F_g = 4$ (7/16 and 9/16) is neglected in the model.

In coated cells, the change in inner state of atoms occurs due to a large number of collisions with walls so that $\tau_g \gg \tau_v$. Hence, at times t from the interval τ_v, $\tau_0 < t \leqslant \tau_g$ atoms entering the laser beam have the equilibrium velocity distribution. However, the distributions integrated over velocity $n_{1,2}(t)$ of the states $|1\rangle$ and $|2\rangle$ relax, as will be shown below, to the resulting stationary state slower with the effective constant $1/T$ which depends on both the interaction with the pump wave and times τ_0 and τ_v.

4.1. Relaxation of populations in coated cells

In the interaction with the pump wave in the time interval $t_0 \leqslant t \leqslant t_0 + \tau_0$, evolution of the populations $\rho_{11}(v,t)$ and $\rho_{22}(v,t)$ of lower states of atom possessing velocity v is described by the following equations

$$\dot{\rho}_{11} = -\dot{\rho}_{22} = -\Gamma(\Delta - kv)\rho_{11}. \qquad (1)$$

The parameter

$$\Gamma(\Delta - kv) = \gamma_2 \frac{|\Omega_1|^2}{(\Delta - kv)^2 + \gamma^2/4}, \qquad (2)$$

where Δ is a detuning from the resonance for atom possessing zero longitudinal velocity and kv is the Doppler frequency shift, presents the rate of transitions from the state $|1\rangle$ to nonabsorbing state $|2\rangle$ through intermediate state $|3\rangle$ under conditions of weak saturation. As was mentioned, at the entry to light field at $t = t_0$ the diagonal elements of the density matrix has the form: $\rho_{11}(v,t_0) = n_1(t_0)f(v)$ and $\rho_{22}(v,t_0) = n_2(t_0)f(v)$. Note that the total normalised populations n_1 and $n_2 = 1 - n_1$ may be considered constant during the interaction period τ_0. Taking the integral over the time τ_0 of flight we obtain the expressions

$$\delta\rho_{11} = -\delta\rho_{22} = -n_1(t_0)f(v)\{1 - \exp[-\Gamma(\Delta - kv)\tau_0]\}, \qquad (3)$$

which describe the variations $\delta\rho_{11,22} = \rho_{11,22}(v, t_0 + \tau_0) - \rho_{11,22}(v,t_0)$ of velocity distribution functions in states $|1\rangle$ and $|2\rangle$. These variations, obviously, have opposite signs. The factor in braces (3) describes local (in the longitudinal velocity) modification of the equilibrium distribution $f(v)$. The parameter $N(\Delta - kv) = \Gamma(\Delta - kv)\tau_0$ in the exponent is the number of transits from state $|1\rangle$ to nonabsorbing state $|2\rangle$ in a time needed for atom to cross the laser field. If $N(\Delta - kv) \sim 1$ then the relative variation of the distribution function for such velocities is on the order of unity.

At a next slower evolution stage, the velocity distributions locally (with respect to $v_z \equiv v$) deformed according to (3) in the result of collisions of atoms with walls relax in time intervals of approximately τ_v to the equilibrium distribution, thus changing the total populations n_1 and $n_2 = 1 - n_1$. Recall that in a coated cell inner atomic states are conserved for a long time τ_g. Since the above mentioned variations are small and occur in a short, as compared to τ_g, time interval $\tau_v \ll \tau_g$ we have

$$\frac{\partial n_1}{\partial t} = \frac{1}{\tau_v}\int \delta\rho_{11}\, dv = -\frac{n_1}{T}. \qquad (4)$$

Here

$$\frac{1}{T} = \frac{1}{\tau_v}\langle 1 - \exp[-\Gamma(\Delta - kv)\tau_0]\rangle, \quad (5)$$

angular brackets denote integration over velocities with the equilibrium distribution $\langle \ldots \rangle \equiv \int dv f(v) \ldots$.

The main contribution to the integral is made by a small vicinity of resonance velocity $v_{res} = \Delta/k$, hence at $|\Delta| \ll kv_T \equiv \omega_D$ the distribution function can be considered constant

$$f(v) \cong \frac{1}{\sqrt{\pi}\, v_T}.$$

Now (5) takes the form

$$\frac{\tau_v}{T} = \frac{\gamma}{\omega_D} F(N/2), \quad (6)$$

where the function

$$F(z) = \sqrt{\pi}\, z e^{-z}[J_0(iz) - iJ_1(iz)] \quad (7)$$

is expressed in terms of the Bessel function of the imaginary argument and the parameter $z = N/2 = \Gamma(0)\tau_0/2 = 2\gamma_2\tau_0(|\Omega_1|/\gamma)^2$ is determined by the optical pumping into the nonabsorbing state for the time needed for atom to cross the field. At raising z, for example, under increasing laser radiation intensity, the function $F(z)$ monotonically increases: $F(z) \sim z$ at $z \ll 1$ and $F(z) \sim \sqrt{z}$ at $z \gg 1$. This means that with an increase in the field intensity $I \sim |\Omega_1|^2$, time T falls first as $1/I$ and then as $1/\sqrt{I}$.

If the optical pumping during the time of flight is approximately unity then

$$T \sim \tau_v \omega_D/\gamma \gg \tau_v, \quad (8)$$

that is, the relaxation time of the total population is greater than τ_v by a factor of $\omega_D/\gamma \gg 1$. Appearance of this parameter is explained by the fact that the pumping deforms velocity distributions in states $|1\rangle$ and $|2\rangle$ only in a small ($\delta v \sim \gamma/k$) range of velocities. These deformations being distributed in a time τ_v over the velocity interval on the order of v_T only result in a small variation of the total population: $\delta n_1/n_1 \sim \delta v/v_T \sim \gamma/\omega_D \ll 1$. A noticeable change in population occurs in the time longer by a factor of ω_D/γ.

In order to describe the population evolution $n_1(t)$ in the time interval extending to $t \sim \tau_g$ it is necessary to introduce the term $(n_2 - n_1)/\tau_g$ to the right-hand side of Eqn (4), which is responsible for the slow process of levelling the populations n_1 and $n_2 = 1 - n_1$ with the characteristic time τ_g. The solution of the resulting equation with the initial condition $n_1(0) = 1/2$ has the form

$$n_1(t) = \frac{1}{2 + \tau_g/T} + \frac{1}{2(1 + 2T/\tau_g)} \exp\left[-\left(\frac{1}{T} + \frac{2}{\tau_g}\right)t\right]. \quad (9)$$

For a cell with a coating, inequality $\tau_g \gg T$ holds. In this case at $t \gg T$ the population reaches the stationary value $n_1 \sim T/\tau_g \ll 1$.

The considered features of parameter T are noticeably revealed in various optical characteristics of resonance gases in cells with antirelaxation coating.

4.2. The transient characteristic of absorption coefficient for running wave

In the insertion of Fig. 2 one can see an experimental transient characteristic for the absorption coefficient of the cell under pulsed switching on of fixed-frequency radiation. The absorption coefficient κ of the pump wave is proportional to the population of upper state $|3\rangle$, averaged over time of flight of atom across the field. In the conditions of weak saturation, the element ρ_{33} of atomic matrix of density is related to ρ_{11} by the relationship $\rho_{33} = (1/\gamma_2)\Gamma(\Delta - kv)\rho_{11}$. By averaging ρ_{11} over the time of flight of atom using (1) and integrating over longitudinal velocity we obtain

$$\kappa(t) \sim \frac{1}{\gamma_2}\frac{n_1(t)}{\tau_0}\langle 1 - \exp[-\Gamma(\Delta - kv)\tau_0]\rangle = \frac{1}{\gamma_2}\frac{\tau_v}{\tau_0}\frac{n_1(t)}{T}. \quad (10)$$

At a final stage of these transformations we used expression (5). The long-term evolution of the absorption coefficient is determined by the function $n_1(t)$, which is given by formula (9). The absorption coefficient reaches a stationary value in a time T, which can be estimated from formula (8). If we take $\tau_v \sim d/v_T$, where d is the transversal dimension of cell, then

$$T \sim \frac{\tau_v \omega_D}{\gamma} \sim \frac{dk}{\gamma}. \quad (11)$$

By substituting $d = 5$ cm and the parameters of $D_{1,2}$-lines $k \approx 7 \times 10^4$ cm^{-1} and $\gamma \approx 3 \times 10^7$ s^{-1} we obtain $T \sim 10$ ms. The stationary value of the absorption coefficient as follows from (9) and (10)

$$\kappa(t \gg T) \sim \frac{\tau_v}{\gamma_2 \tau_0 \tau_g} \quad (12)$$

is proportional to a simple combination of three characteristic times τ_0, τ_v, and τ_g.

The results obtained – a reduction of time T at growing radiation intensity, relationship (6), estimate (11) of its characteristic value at $N \sim 1$, and independence of the value of stationary absorption on intensity – agree with the experimental results (see insertion in Fig. 2).

4.3. Absorption of probe wave in scanning the laser radiation frequency

The counterpropagating probe and the pump waves vary linearly in time

$$\Delta(t) = \frac{\Delta_0}{\tau_0} t, \quad (13)$$

where Δ_0 is the frequency variation (for definiteness positive) for the time τ_0 of flight of atom across the laser beam. Thus, at $\Delta_0 \sim \gamma$ a Doppler-free resonance is detected in time τ_0. The time needed to record the whole Doppler profile is determined from the condition $|\Delta(t)| = \omega_D$, that is, $|t| = t_D \equiv \omega_D \tau_0/\Delta_0$. At $\Delta_0 \sim \gamma$ we obtain $t_D \sim (\tau_0/\tau_v)T < T$, that is, for the total time of scanning the system is not saturated due to interaction with the pump wave. Further on, we assume $\Delta_0 = \gamma$ because this considerably simplifies explicit forms of analytical expressions and by the order of magnitude corresponds to the rate of frequency variation in the experiment except for, obviously, the limiting cases of fast (presented in Fig. 5) or slow scanning.

When the field frequency is varied, the dependence of T on time is determined by the expression

$$\frac{\tau_v}{T(t)} = \left\langle 1 - \exp\left\{-\frac{N}{2}\arctan 2\left[\frac{\Delta(t) - kv}{\gamma}\right]^2\right\}\right\rangle, \quad (14)$$

from which one can see that $1/T(t)$ is a monotonically decreasing function of $|t|$. In the range $|t| \ll t_D$ it actually remains

constant, whereas at $|t| > t_D$ it exponentially decreases. If $N \sim 1$ then in the range $|t| \leqslant t_D$ the characteristic value of $T \sim \tau_v \omega_D/\gamma$ coincides with estimate (8). Note that at $|t| \ll t_D$ and $N \ll 1$ formula (14) coincides with results (6), (7).

From (4) one can see that evolution of $n_1(t)$ in view of dependence $T(t)$ is as follows:

$$n_1(t) = \frac{1}{2}\exp\left[-\int_0^\infty \frac{d\tau}{T(t-\tau)}\right]. \quad (15)$$

For simplicity we assumed $t \leqslant T \ll \tau_g$. In the course of frequency scanning the population $n_1(t)$ monotonically decreases from $n_1(-\infty) = 1/2$ to

$$n_1(\infty) = \frac{1}{2}\exp\left[-\int_0^\infty \frac{dt}{T(t)}\right],$$

where the integral in the exponent is equal by the order of magnitude to $t_D/T \sim \tau_0/\tau_v < 1$ so that there is no strong depletion of the lower working level.

The absorption coefficient for a weak probe wave calculated by the perturbation theory is proportional to

$$\kappa_2(t) \sim n_1(t)\left\langle \frac{1}{\tau_0}\int_{-\tau_0/2}^{\tau_0/2} \frac{d\tau\,|\Omega_2|^2}{[\Delta(t+\tau)+kv]^2+\gamma^2/4} \right.$$

$$\left. \times \exp\left\{-\int_{-\tau_0/2}^{\tau} \frac{d\tau'\gamma_2\,|\Omega_1|^2}{[\Delta(t+\tau')-kv]^2+\gamma^2/4}\right\}\right\rangle. \quad (16)$$

Here the integral over τ presents averaging with respect to time of flight of the product of two terms: one related with the action of the probe field (Ω_2) and second pertaining to the accumulating effect of interaction between the pump wave (Ω_1) and atoms possessing a longitudinal velocity v. The population $n_1(t)$ weakly varies during the time of flight and is therefore considered constant in averaging over τ. Expression (16) describes evolution of the absorption coefficient in the whole range of frequency scanning. To analyse experimentally observed specific features it suffices to consider the limiting cases of large and small detunings $|\Delta(t)|$.

In the range $|\Delta(t)| \gg \gamma$a, that is, far from the Doppler-free resonance formula (16) takes the form

$$\kappa_2(t) \sim 2\sqrt{\pi}\frac{|\Omega_2|^2}{\gamma\omega_D} n_1(t)\exp\left[-\frac{\Delta^2(t)}{\omega_D^2}\right]. \quad (17)$$

Note that function $n_1(t)$ in this expression is related to the action of the pump wave and substantially changes in the time interval on the order of frequency scanning duration. By differentiating (17) with respect to t we obtain

$$\frac{d\kappa_2}{dt} \sim n_1\exp\left[-\frac{\Delta^2(t)}{\omega_D^2}\right]\left\{-\frac{1}{T(t)} - \frac{1}{\omega_D^2}\frac{d\Delta^2}{dt}\right\}. \quad (18)$$

The expression in braces turns to zero at point t_0 satisfying the condition

$$t_0\,T(t_0) = -\frac{1}{2}\left(\frac{\tau_0\omega_D}{\gamma}\right)^2 < 0, \quad (19)$$

that is, the maximal absorption is attained earlier than the Doppler-free resonance is observed, which occurs at $t = 0$. This result, obviously, is independent of the sign of frequency tuning. If $T \sim \tau_v\omega_D/\gamma$ then $|t_0| \sim (\tau_0/\tau_v)t_D$, that is, the maximal absorption is realised within the time of scanning and $|\Delta(t_0)| \sim \tau_0\omega_D/\tau_v \gg \gamma$. From (17) one can see that the shift of maximal absorption is caused by two competing factors: the decreasing population of the working level $|1\rangle$ due to optical pumping and increasing probability of absorption while approaching the centre of line. These results agree with the experimental data presented in Fig. 4. Note that at higher scanning rate Δ_0/τ_0, which we assumed equal to γ/τ_0, the shift $|t_0|$ decreases proportionally to $(\tau_0/\Delta_0)^2$. Hence, at sufficiently high scanning rate where the time of passing the line becomes noticeably less than T, the shift of the maximal absorption relative to the undisturbed atomic frequency actually vanishes, which agrees with the experimental curve presented in Fig. 5.

In describing the Doppler-free resonance we may consider the absorption coefficient (17) near $t = 0$ where $|\Delta(t)| \ll \gamma$. Assume, in addition, that $N \ll 1$. Then for $\kappa_2(t)$ we obtain

$$\kappa_2(t) \sim 2\sqrt{\pi}\frac{|\Omega_2|^2}{\gamma\omega_D} n_1(0)\left[1 + \frac{N\Delta^2(t)}{\gamma^2}\right], \quad (20)$$

which means that the absorption coefficient has a local minimum at the line centre, that is, at point $t = 0$, where the detuning is $\Delta = 0$. The local minimum at the centre of the absorption line just reveals the appearance of a Doppler-free resonance.

Thus, the theory in this section well describes experimentally observed features of the transient and spectral characteristics of absorption in cells with a coating in scanning the frequency of the laser field.

5. Conclusions

Specific features of laser radiation absorption in resonance lines of Cs atoms are studied in cells with antirelaxation coating. It was established that high-contrast Doppler-free resonances may be formed in such cells despite the loss of selectivity of optical pumping with respect to longitudinal velocity in collisions with walls. In the approximation of three-level theoretical model, most of observed effects were explained and a qualitative interpretation was made. A series of effects are beyond the framework of this article, those are connected with the optical pumping to nonabsorbing Zeeman sub-levels, influence of circular polarisation, magnetic field orientation, and phase noise of laser radiation. These important effects are studied in the framework of developing an energy-efficient laser magnetometer and will be described in a future publication.

Acknowledgements. The work was supported by the Ministry of Education and Science of the Russian Federation (State Contract No. 12.527.12.5007 dated 14.06.2012).

References

1. Demtreder W. *Laser Spectroscopy* (New York: Springer, 2003).
2. Pappas P.G., Burns M.M., Hinshelwood D.D., Feld M.S. *Phys. Rev. A*, **21**, 1955 (1980).
3. Pomerantsev N.M., Ryzhov V.M., Skrotskii G.V. *Fizicheskie osnovy kvantovoi magnitometrii* (Physical Foundations of Quantum Magnetometry) (Moscow: Nauka, 1972).
4. Budker D., Romalis M. *Nature Phys.*, **3**, 227 (2007).
5. Aleksandrov E.B., Vershovskii A.K. *Usp. Fiz. Nauk*, **179**, 605 (2009).
6. Kominis I.K., Kornack T.W., Allred J.C., Romalis M.V. *Nature*, **422**, 596 (2003).

7. Vanier J., Audoin C. *The Quantum Physics of Atomic Frequency Standards* (Bristol – Philadelphia: Adam Hilger, 1989).
8. Budker D., Hollberg L., Kimball D.F., Kitching J., Pustelny S., Yashchuk V.V. *Phys. Rev. A*, **71**, 012903-1-9 (2005).
9. Groeger S., Pazgalev A.S., Weis A. *Appl. Phys. B*, **80**, 645 (2005).
10. Kholodov Yu.A., Kozlov A.N., Gorbach A.M. *Magnitnye polya biologicheskikh ob'ektov* (Magnetic Fields of Biological Objects) (Moscow: Nauka, 1987).
11. Bison G. et al. *Intern. Congress Ser.*, **1300**, 561 (2007).
12. Vasiliev V., Zibrov S.A., Velichansky V.L. *Rev. Sci. Instrum.*, **77**, 013102 (2006).
13. Bykovskii Yu.A., Velichansky V.L., Maslov V.A., Egorov V.K. *Pis'ma Zh. Eksp. Teor. Fiz.*, **19**, 665 (1974).
14. Zibrov S.A., Dudin Ya.O., Radnaev A.G., Vasil'ev V.V., Velichansky V.L., Brazhnikov D.V., Taichenachev A.V., Yudin V.I. *Pis'ma Zh. Eksp. Teor. Fiz.*, **85**, 515 (2007).
15. Vasil'ev V.V., Velichansky V.L., Zibrov S.A., Sivak A.V., Brazhnikov D.V., Taichenachev A.V., Yudin V.I. *Zh. Eksp. Teor. Fiz.*, **139**, 883 (2011).